Structural Determinants of Fluoride and Formate Binding to Hemoglobin and Myoglobin: Crystallographic and ^{1}H-NMR Relaxometric Study

Silvio Aime,* Mauro Fasano,* Silvia Paoletti,* Francesca Cutruzzolà,‡ Alessandro Desideri,§ Martino Bolognesi,¶‖ Menico Rizzi,‖ and Paolo Ascenzi**

*Department of Inorganic, Physical and Materials Chemistry, University of Turin, 10125 Turin; ‡Department of Biochemical Sciences "Alessandro Rossi Fanelli," University of Rome "La Sapienza," 00185 Rome; §Department of Organic Chemistry and Biochemistry, University of Messina, Salita Sperone, 98100 Messina; ¶I.S.T. Biostructure Unit, Department of Physics, University of Genoa, 16132 Genoa; ‖Department of Genetics and Microbiology, University of Pavia, 27100 Pavia; and **Department of Pharmaceutical Chemistry and Technology, University of Turin, 10125 Turin, Italy

ABSTRACT The x-ray crystal structure of the fluoride derivative of ferric sperm whale (*Physeter catodon*) myoglobin (Mb) has been determined at 2.5 Å resolution ($R = 0.187$) by difference Fourier techniques. The fluoride anion, sitting in the central part of the heme distal site and coordinated to the heme iron, is hydrogen bonded to the distal His(64)E7 NE2 atom and to the W195 solvent water molecule. This water molecule also significantly interacts with the same HisE7 residue, which stabilizes the coordinated fluoride ion. Moreover, fluoride and formate binding to ferric *Aplysia limacina* Mb, sperm whale (*Physeter catodon*) Mb, horse (*Caballus caballus*) Mb, loggerhead sea turtle (*Caretta caretta*) Mb, and human hemoglobin has been investigated by ^{1}H-NMR relaxometry. A strong solvent proton relaxation enhancement is observed for the fluoride derivatives of hemoproteins containing HisE7. Conversely, only a small outer-sphere contribution to the solvent relaxation rate has been observed for all of the formate derivatives considered and for the *A. limacina* Mb:fluoride derivative, where HisE7 is replaced by Val.

INTRODUCTION

Oxygen-carrying heme proteins share a highly conserved three-dimensional structure, despite low levels of sequence homology (Bashford et al., 1987).

The heme-iron ligand stabilization mechanism in heme proteins has been widely investigated, for ligands of both ferrous and ferric forms. Ligand binding to heme proteins is controlled by structural determinants (i.e., specific amino acid residues) either present in the heme pocket and/or far from the heme but functionally linked to it through an allosteric mechanism (Brunori et al., 1989; Perutz, 1989, 1990; Conti et al., 1993; Ansari et al., 1994; Brancaccio et al., 1994; Springer et al., 1994; Smerdon et al., 1995). The key role of the highly conserved distal HisE7 residue in controlling ligand binding processes has been established through a number of structural, thermodynamic, and kinetic studies on naturally occurring and properly engineered heme proteins. In this respect, in *Aplysia limacina* myoglobin (Mb), the absence of the distal HisE7 (replaced by Val) is partially compensated for by the presence of an arginyl residue at position E10, which upon ligand binding has been shown to fold into the distal site, triggering the formation of extended polar interactions that stabilize the heme iron-bound ligand. And in sperm whale (*Physeter catodon*) Mb mutants, removal of HisE7 is partially compensated for by introduction of an arginyl residue at position E10. Moreover, in ferric heme proteins, water molecule(s) may participate to stabilize the heme iron-bound ligand through a network of hydrogen bonds involving amino acid residues (Perutz, 1989; Conti et al., 1993; Brancaccio et al., 1994; Springer et al., 1994; Smerdon et al., 1995).

To gain more insight into the understanding of the ligand recognition processes operating in heme proteins, we investigated the fluoride and formate binding mode to *A. limacina* Mb, horse (*Caballus caballus*) Mb, sperm whale (*Physeter catodon*) Mb, loggerhead sea turtle (*Caretta caretta*) Mb, and human hemoglobin (Hb) by x-ray crystallography and ^{1}H-NMR relaxometric techniques. The presence of a water molecule close to HisE7 and hydrogen bonded to the heme coordinated fluoride anion (Deatherage et al., 1976; Fermi and Perutz, 1977; Perutz, 1979), which was just supposed to be present based on measurements in solution (Fabry and Eisenstadt, 1974; Koenig et al., 1981; Oakes, 1986; Aime et al., 1993, 1995), has now been definitely assessed. On the other hand, in *A. limacina* Mb, bearing Val(63)E7, the fluoride anion is hydrogen bonded only to the Arg(66)E10 side chain (Bolognesi et al., 1990; Conti et al., 1993), and there are no water molecules in closest proximity to the heme-iron bound ligand.

The results reported herein outline the role of amino acid residues present at positions E7 and E10, playing a stabilizing role not only on the heme-bound ligand, but also on the water molecule hydrogen bonded to it. Moreover, the latter water molecule provides an interpretation for the strong enhancement of the water proton NMR relaxation rate in ferric hemoprotein solutions upon fluoride binding reported earlier (Fabry and Eisenstadt, 1974; Vuk-Pavlovic et al., 1977; Koenig et al., 1981; Oakes, 1986).

Received for publication 26 July 1995 and in final form 29 September 1995.

Address reprint requests to Dr. Silvio Aime, Department of Inorganic, Physical and Materials Chemistry, University of Turin, Via Pietro Giuria 7, 10125 Turin, Italy. Tel.: +39-11-6707520; Fax: +39-11-6707524; E-mail: aime@silver.ch.unito.it.

0006-3495/96/01/482/07 $2.00

MATERIALS AND METHODS

Hemoproteins and chemicals

A. limacina Mb and *C. caretta* Mb were prepared as detailed elsewhere (Conti et al., 1993; Nardini et al., 1995). Horse heart Mb and sperm whale Mb were obtained from Sigma Chemical Co. (St. Louis, MO). Human adult Hb was prepared according to the method of Antonini and Brunori (1971). The characterization of the hemoproteins considered has previously been reported (Antonini and Brunori, 1971; Conti et al., 1993; Nardini et al., 1995). All chemicals, from Merck AG (Darmstadt, Germany), were of analytical grade and were used without further purification.

X-ray crystallography

Preparation of the fluoride derivative of sperm whale Mb was achieved by soaking the ferric protein crystals (Takano, 1977) in their mother liquor solution containing 0.2 M NaF (50 mM phosphate buffer, pH = 7.1) at 20°C for 12 h. Diffracted intensities for the fluoride derivative of ferric sperm whale Mb were collected on a Rigaku R-axis II image plate system, using CuKα radiation. For the fluoride derivative 8596 independent reflections were collected and reduced to 3742 unique reflections (R_{merge} = 9.0%, completeness 80% in the 15 to 2.5 Å resolution range).

On the basis of the refined coordinates of native ferric sperm whale Mb (Takano, 1977), the structure of the fluoride adduct was examined by difference Fourier techniques. Calculation of the $2F_d$-F_n and F_d-F_n difference electron density maps (where F_d is the structure factor amplitude for the fluoride derivative, and F_n is the amplitude for the native ferric protein) with calculated phases (the distal histidine residue and the distal site water molecule were omitted from phase calculation) allowed us to immediately locate the ligand and a water molecule in the heme distal site. The protein model was refined using X-PLOR (Brünger, 1990); a total of 200 cycles of energy mimimization were run. Fluoride and the W195 water molecule were fitted to their electron density at this stage (R = 0.187; 15 to 2.5 Å data) using the program FRODO (Jones, 1978). Attainment of convergence was evaluated by examination of the coordinate root mean square deviations between cycles, and through inspection of difference electron density maps.

The three-dimensional structures of the fluoride derivative of ferric *A. limacina* Mb and adult human Hb (Deatherage et al., 1976; Fermi and Perutz, 1977; Bolognesi et al., 1990; Conti et al., 1993) as well as of the formate derivative of *C. caretta* Mb (Leci et al., 1995) have been reported previously.

Amino acid residues have been identified by their three-letter code, their sequence number (within parentheses), and their topological position within the eight helices of the globin fold (Perutz, 1979). For the numbering of the heme group atoms, the scheme of Takano (1977) has been adopted.

NMR theory

The longitudinal relaxation rate of solvent water protons of solutions containing paramagnetic hemoproteins (Bertini and Luchinat, 1986; Banci et al., 1991) is given by Eq. 1,

$$R_{1obs} = R_{1p} + R_{1d} + R_1^{w} \tag{1}$$

where R_1^{w} is the relaxation rate of pure water, and R_{1p} and R_{1d} are, respectively, the paramagnetic and the diamagnetic relaxation contributions from the metalloprotein. R_{1p} is easily determined by subtracting from the observed relaxation rate the relaxivity value measured for solutions containing a diamagnetic derivative of the same hemoprotein or of a similar diamagnetic protein. R_{1p} is the sum of inner- (R_{1p}^{is}) and outer- (R_{1p}^{os}) sphere contributions.

The inner-sphere relaxation rate is accounted for in terms of the following set of equations (Eqs. 2–4) (Bertini and Luchinat, 1986), widely used to describe aqueous solutions of paramagnetic metal ions:

$$R_{1p}^{is} = q/111 \cdot \frac{1}{T_{1M} + \tau_M} \tag{2}$$

$$T_{1M}^{-1} = 2/15 \frac{\gamma H^2 g^2 \mu_B^2 S(S+1)}{r^6} \times \left(\frac{7\tau_c}{1 + \omega_S^2 \tau_c^2} + \frac{3\tau_c}{1 + \omega_H^2 \tau_c^2} \right) \tag{3}$$

$$\tau_c^{-1} = \tau_R^{-1} + \tau_M^{-1} + \tau_s^{-1} \tag{4}$$

In Eqs. 2–4, q is the number of exchangeable protons, τ_M is their mean residence lifetime, T_{1M} is their longitudinal relaxation time, S is the electron spin quantum number, γ_H is the proton nuclear magnetogyric ratio, g and μ_B are the electronic Landé factor and the Bohr magneton, respectively, r is the distance between the metal ion and the protons, ω_H and ω_S are the proton and electron Larmor frequencies, respectively, τ_R is the reorientational correlation time, and τ_s is the longitudinal electron spin relaxation time.

The outer-sphere contribution to the overall relaxation rate is usually described in terms of the diffusion-controlled dipolar relaxation theory (Eqs. 5–8). Although this theory refers to relaxation in dilute solutions of small paramagnetic compounds (Hwang and Freed, 1975), we may use this approach to describe the outer-sphere relaxation in hemoprotein solutions from a phenomenological point of view.

$$R_{1p}^{os} = (32\pi/405)\, \gamma_H^2 g^2 \mu_B^2 \times S(S+1)\, (N_A/1000)(M/aD)[7J(\omega_S) + 3J(\omega_I)] \tag{5}$$

$$J(\omega) = \frac{1 + 5z/8 + z^2/8}{1 + z + z^2/2 + z^3/6 + 4z^4/81 + z^5/81 + z^6/648} \tag{6}$$

$$z = 2(\omega\tau_D + \tau_D/\tau_s)^{1/2} \tag{7}$$

$$\tau_D = a^2/D \tag{8}$$

In Eqs. 5–8, N_A is Avogadro's number, M is the concentration of the paramagnetic molecule, a is the distance of closest approach of outer-sphere water molecules to the paramagnetic center, and D is the sum of the diffusion coefficients of solute and water molecule. τ_D, as described by Eq. 8, is the translational diffusion correlation time (the approximate time for solute and solvent to diffuse apart).

NMR measurements

Single-frequency T_1 measurements of all the hemoprotein solutions (in 0.050 M phosphate buffer, pH 6.5) were obtained on a Stelar SpinMaster Spectrometer (Stelar, Mede (PV), Italy) operating at 20 MHz, by means of the usual inversion-recovery technique (16 experiments, four scans) (Friebolin, 1993). A typical 90° pulse width was 3.5 μs. The τ values were linearly increased from a starting value corresponding to one-seventh of the estimated null point ($0.693 \cdot T_1$), so that the null point occurs on the middle of the inversion-recovery curve (7th experiment). In the 16th experiment the free induction decay is acquired after a single 90° pulse, to get the M_∞ value. The reproducibility in T_1 measurements was ±0.5%. The temperature was controlled by a Stelar VTC91 variable temperature controller, equipped with a copper-constantan thermocouple; the actual temperature in

the probe head was measured with a Fluke 52 k/j digital thermometer, with an uncertainty of ±0.3°C.

R_{1p} values have been determined by subtracting from the observed relaxation rate (R_1^{obs}) the diamagnetic relaxivity value (R_1^{dia}) measured for solutions containing a diamagnetic derivative of a similar hemoprotein (such as human HbO_2) at the same concentration. Here, the following R_1^{dia} values, measured at 1.0 mM human HbO_2 concentration, have been used: 0.69 s^{-1} (5°C), 0.61 s^{-1} (10°C), 0.54 s^{-1} (15°C), 0.47 s^{-1} (20°C), 0.42 s^{-1} (25°C), 0.37 s^{-1} (30°C), 0.33 s^{-1} (35°C), 0.29 s^{-1} (40°C), 0.26 s^{-1} (45°C). Values of R_1^{dia} for the oxygenated derivative of *A. limacina* Mb, horse Mb, sperm whale Mb, *C. caretta* Mb, and human Hb do not display significant differences. R_1^{dia} values at other temperatures have been graphically extrapolated from a plot of these points.

The $1/T_1$ nuclear magnetic relaxation dispersion (NMRD) profiles of water protons were measured at variable temperature over a continuum of magnetic fields from 0.00024 to 1.2 *T* (corresponding to 0.01 to 50 MHz proton Larmor frequency) on the Koenig-Brown field-cycling relaxometer (Koenig and Brown, 1990) installed at the Department of Chemistry of the University of Florence (Italy). The relaxometer works under complete computer control with an absolute uncertainty in $1/T_1$ of ± 1%. The temperature was controlled using a circulating bath of a perhalogenated hydrocarbon and was actually determined in the probe head with a mercury thermometer near the sample tube.

RESULTS AND DISCUSSION

At the end of the refinement, the *R*-factor for the ferric sperm whale Mb:fluoride adduct is 0.187 (for the data in the 15 to 2.5 Å resolution range). Deviations from ideality of 0.017 Å for bond lengths and of 2.9° for bond angles were observed. The model contains 1216 protein atoms, 123 water molecules, and the monoatomic ligand.

Fluoride is coordinated to the heme iron, the Fe-ligand distance being 2.23 Å (see Figs. 1 and 2 *A*). Moreover, the anionic ligand is hydrogen bonded to the distal His(64)E7 NE2 atom (2.74 Å) and to the W195 water molecule, deeply buried in the distal site of the heme cavity (2.71 Å). The W195 water molecule is at 3.83 Å from the distal His(64)E7 NE2 atom. The iron is contained in the heme plane (the out-of-plane distance calculated with respect to the four pyrrole nitrogens is 0.02 Å, toward the proximal side). The His(93)F8 NE2-Fe coordination distance is 2.47 Å.

The fluoride binding mode to sperm whale Mb (Figs. 1 and 2 *A*) is reminiscent of that observed for human Hb (Deatherage et al., 1976; Fermi and Perutz, 1977; Perutz, 1979). A different structural organization upon fluoride binding is observed in *A. limacina* Mb (Bolognesi et al., 1990; Conti et al., 1993) (see Fig. 2 *B*), where the highly conserved HisE7 distal residue is replaced by Val, and fluoride is hydrogen bonded to the Arg(66)E10. Moreover, no water molecules are observed within hydrogen bonding distance from the heme iron coordinated fluoride in *A. limacina* Mb (the nearest water molecule, W211, is 7.3 Å away from the fluoride, on the entrance of the distal pocket). The different fluoride binding modes found in the crystal structures of sperm whale Mb, *A. limacina* Mb and human Hb are consistent with solution-state behavior, as assessed by NMR relaxometric measurements.

Upon fluoride binding to ferric human Hb, sperm whale Mb, horse Mb, and *C. caretta* Mb, a very strong relaxation enhancement is observed (Koenig et al., 1981; Oakes, 1986; Aime et al., 1993, 1995). On the other hand, a very small relaxation enhancement of solvent water protons is observed when fluoride binds to ferric *A. limacina* Mb. The observed behavior is different from that reported by Fabry and Eisenstadt (1974) for *Aplysia californica* Mb.

Fig. 3 *A* shows the ligand binding isotherms for fluoride association to the hemoproteins considered, observed by measurement of the paramagnetic contribution to the solvent water proton relaxation rate. The hyperbolic behavior of the binding isotherms provides the value of the association equilibrium constant (K_a). K_a values obtained by means of the NMR relaxometric method are reported in Table 1 and agree very well with those reported in the literature, obtained by spectrophotometric methods.

On the basis of Eq. 2, we would expect that the displacement of the heme-bound water molecule in ferric human Hb, sperm whale Mb, horse Mb, and *C. caretta* Mb by the fluoride ion would cause a reduction of the paramagnetic contribution to the overall water proton relaxation rate. Such a reduction was actually observed as the hemoprotein solutions were titrated with sodium formate (Fig. 3 *B*), which is known to replace the fluoride ion in terms of both coordination geometry (formate acts as a monodentate ligand) and magnetic moment (Antonini and Brunori, 1971; Leci et al., 1995). Again, the fitting procedure of these data provides K_a values for the ferric hemoprotein-formate adducts, which agree very well with those reported in the literature (Table 1).

The observed relaxation enhancement upon fluoride coordination may be accounted for in terms of an increase in both the effective magnetic moment and the electronic relaxation time τ_s (Fabry and Eisenstadt, 1974; Gupta and Mildvan, 1975), with a consequent increase of the diffusion-

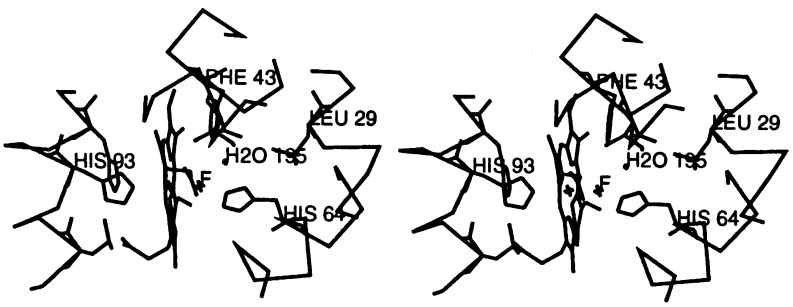

FIGURE 1 Stereo view of the heme pocket in the sperm whale Mb:fluoride adduct. The heme group; Leu(29)B10, Phe(43)CD1, His(64)E7, and His(93)F8 residues; the coordinated fluoride anion (F); and the W195 water molecule (H_2O 195) are shown.

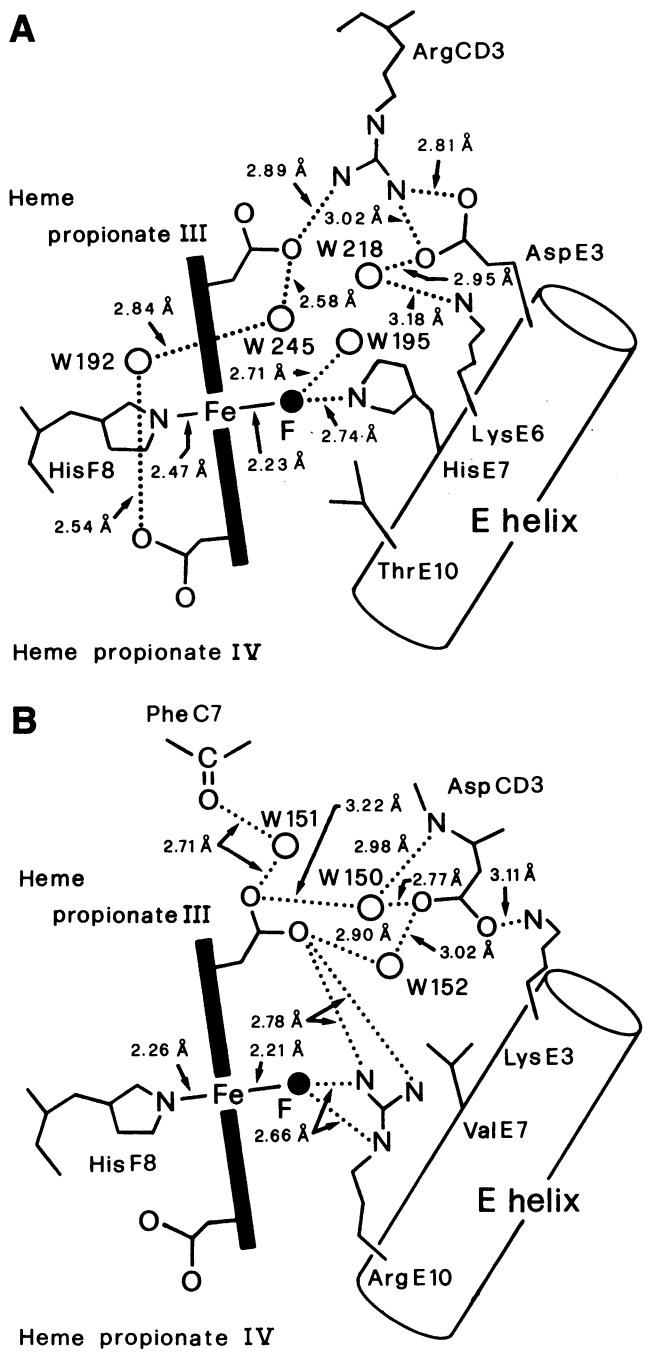

FIGURE 2 Schematic cartoons of the three-dimensional models of the fluoride derivative of ferric sperm whale Mb (*A*) and *A. limacina* Mb (*B*; modified from Conti et al., 1993). Ordered water molecules are represented by open circles, fluoride ligand by a filled circle, and hydrogen bonds by dotted lines. The distance between W195 and HisE7 NE2 in *A* is 3.83 Å.

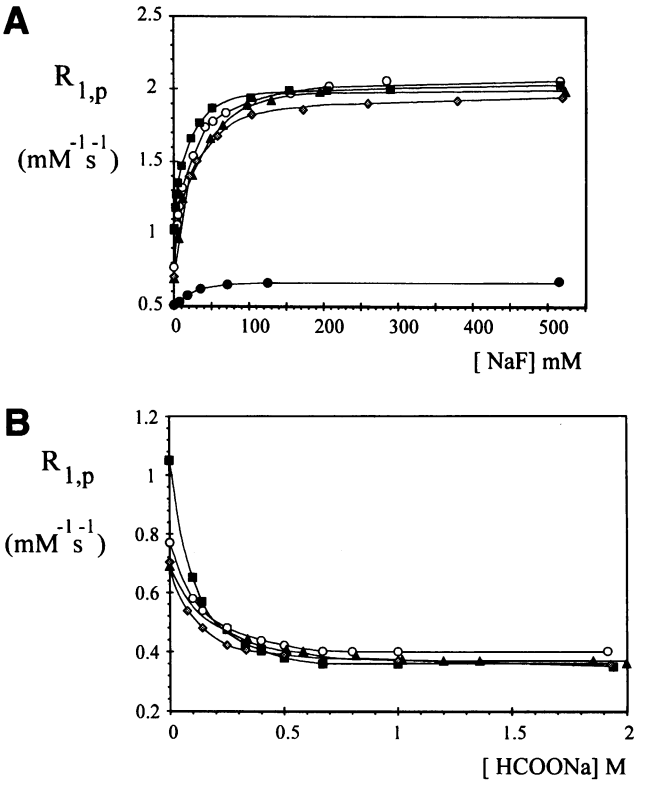

FIGURE 3 Paramagnetic contribution to the solvent water proton relaxation rate in 1.0 mM (expressed as heme content) hemoprotein solutions at pH 6.5, 25°C, and 20 MHz versus fluoride (*A*) and formate (*B*) concentrations. ○, horse Mb; ■, sperm whale Mb; ▲, human Hb; ◆, *C. caretta* Mb; ●, *A. limacina* Mb.

controlled dipolar relaxation of solvent water protons. However, it is now clear enough that the major cause for the strong relaxation enhancement in fluoride derivatives is actually the short distance of the water molecule in the second coordination sphere (Koenig et al., 1981; Aime et al., 1995); indeed, this water molecule is kept in close proximity to the paramagnetic center long enough to let the water nuclei experience a fluctuating dipolar interaction that is no longer modulated (controlled) by the solute-solvent reciprocal diffusion (Banci et al., 1991).

To gain more insight into the operating mechanism responsible for the observed increase in overall relaxivity, we resorted to field-cycling relaxometry (Noack, 1986; Koenig and Brown, 1990), which is the technique of choice for obtaining information on both structural and dynamic properties of paramagnetic metalloproteins and complexes.

Fig. 4 shows the $1/T_1$ NMRD profiles of ferric human Hb, horse Mb, sperm whale Mb, and *A. limacina* Mb fluoride derivatives at 25°C. As expected, remarkably different NMRD profiles have been observed for *A. limacina* Mb ($q = 0$) and the other hemoproteins considered. As shown by the low relaxivity values measured in the *A. limacina* Mb solution at any frequency, the outer-sphere contribution to the overall solvent proton relaxation rates is quite small.

NMRD data for the fluoride derivative of ferric hemoproteins cannot be quantitatively analyzed in terms of Eq. 3 because of the presence of a large zero field splitting (ZFS) (Fann et al., 1995). When the ZFS energy is larger than $h\tau_s^{-1}$, a large fraction of the low field relaxivity is quenched because some of the electron transitions occur at a frequency much higher than the electron Larmor frequency (Banci et al., 1991). Only at B_0 values greater

TABLE 1 Values of the association equilibrium constant* for fluoride and formate binding to ferric monomeric and tetrameric heme proteins

Heme protein	Fluoride	Formate
Sperm whale Mb	6.0×10^{1}‡	1.0×10^{1}§
	8.0×10^{1}¶	*1.0×10^{1}*¶
Horse Mb	6.3×10^{1}‖	1.0×10^{1}‖
	8.3×10^{1}¶	*9.4*¶
C. caretta Mb	7.1×10^{1}**	1.3×10^{1}§
	5.7×10^{1}¶	*1.1×10^{1}*¶
Human Hb	5.9×10^{1}‡‡	1.1×10^{1}**
	4.4×10^{1}¶	*8.1*¶
A. limacina Mb	1.0×10^{2}§§	1.1§
	4.3×10^{1}¶	*n.d.*¶¶

*Association equilibrium constants are M^{-1}. Values reported in italics have been obtained with ^{1}H-NMR relaxometry.
‡pH 7.0, 22°C. From Conti et al. (1993).
§pH 7.0, 20°C. From Leci et al. (1995).
¶pH 6.5, 25°C. Present study.
‖pH 7.0, 22°C. From Antonini and Brunori (1971).
**pH 7.0, 20°C. P. Ascenzi, unpublished results.
‡‡pH 7.5, 20°C. From Antonini and Brunori (1971).
§§pH 7.0, 20°C. From Conti et al. (1993).
¶¶n.d., not detectable with ^{1}H NMR relaxometric measurement: the relaxivity of ferric *A. limacina* Mb solution does not change upon addition of sodium formate (see text).

than $2D/g_e\mu_B$ (D being the ZFS energy) is the NMRD profile expected to match that predicted by the Solomon theory (Banci et al., 1991). High spin iron (III) experiences a relatively large spin-orbit coupling, which is expected to cause a short electronic relaxation time τ_s. Indeed, the temperature independence of the NMRD profiles of both sperm whale and horse Mb:fluoride adducts indicates that the correlation time for the fluctuation of the dipolar interaction cannot be the reorientational correlation time. Hence, τ_s is shorter than τ_R at any temperature and frequency. The observed temperature independence is also evidence that the water molecule responsible for the enhancement is in fast exchange with bulk water (i.e., $\tau_M < 0.1$ μs at any considered temperature, so as not to influence the measured profiles). A NMRD profile has been calculated with the Solomon theory (Eqs. 2–4), using an average iron-proton distance of 3.6 Å (from x-ray data), a short exchange lifetime ($\tau_M = 0.1$ μs), and the reorientational correlation time ($\tau_R =$ 5.5 ns) reported in the literature for deoxy-Mb (Bertini and Luchinat, 1986; p.196). A "phenomenological" outer sphere was simulated to obtain a contribution similar to that of the ferric derivative of *A. limacina* Mb, and an electronic relaxation time in the range of 20 to 60 ps was chosen, so as to be the shortest among the different correlation times. As shown in Fig. 5, there is a very good agreement between the actual measurement (here for horse Mb:fluoride adduct) and the calculated profile in the frequency range from 2 to 50 MHz, where the spin-orbit coupling mechanism is no longer effective.

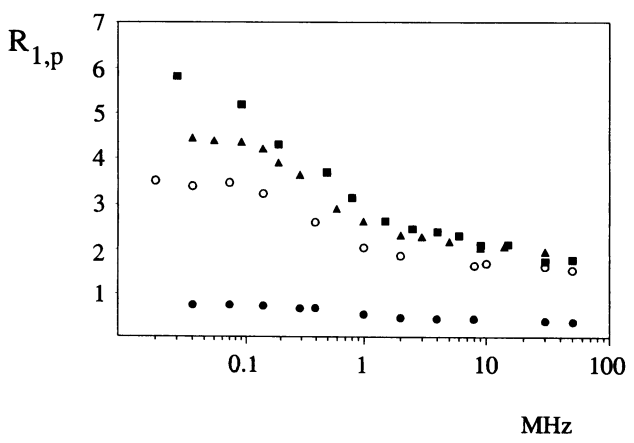

FIGURE 4 $1/T_1$ NMRD profiles of 1.0 mM (expressed as heme content) hemoprotein:fluoride adduct solutions at pH 6.5 and 25°C. Sodium fluoride was about 1 M, i.e., under conditions approaching saturation. Observed rates have been subtracted by the diamagnetic (1.0 mM HbO_2) contribution. ○, horse Mb; ■, sperm whale Mb; ▲, human Hb; ●, *A. limacina* Mb.

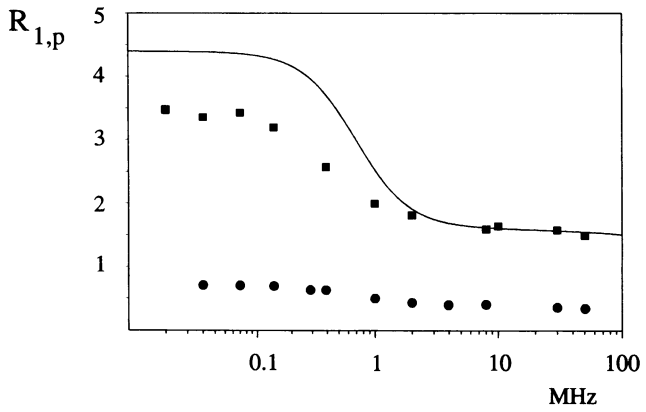

FIGURE 5 Experimental (■) and calculated (*line*) $1/T_1$ NMRD profile of 1.0 mM horse Mb at 25°C. Filled circles are experimental measurements on the *A. limacina* Mb:fluoride solution (see Fig. 4) used for calculating the outer-sphere contribution to the profiles. The best-fitted value for the electronic relaxation time is 35 ps. For details and value of other parameters used in the simulation see text.

In the case of the human Hb:fluoride complex, a significant decrease of $R_{1,p}$ values is observed on the low frequency side of the $1/T_1$ NMRD profiles upon decreasing the temperature from 25°C to 5°C (Fig. 6). This reduction clearly reflects the elongation of τ_M at lower temperatures, and it takes place only when T_{1M} becomes noticeably shorter (see Eq. 2), i.e., at low frequencies. Consequently, we calculate a τ_M value of 2×10^{-6} s at room temperature from low field $R_{1,p}$ data by assuming that $T_{1M} = \tau_M$. The different behavior of human Hb with respect to Mb's lies then in the fact that the former species is still reminiscent of the long exchange lifetime shown by the parent ferric form. As previously anticipated (Aime et al., 1993), the relatively long exchange lifetime of the heme iron bound water molecule in hemoproteins is largely due to the restricted mobility of water molecules in the exchange pathway from the heme cavity to the bulk solvent.

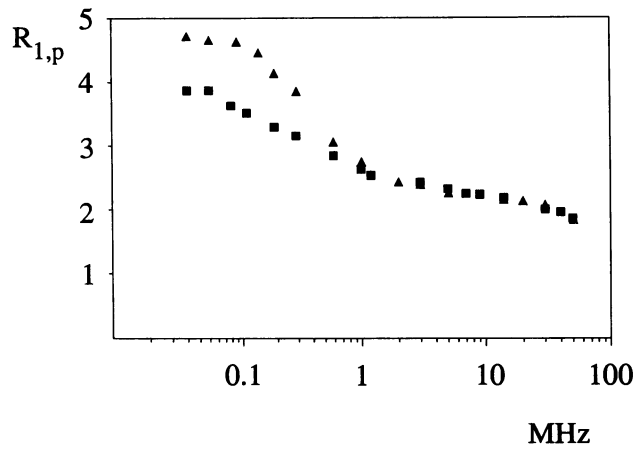

FIGURE 6 $1/T_1$ NMRD profiles of a 1.0 mM (expressed as heme content) human Hb:fluoride solution at 5°C (■) and 25°C (▲). Other experimental conditions as in Fig. 4. Observed relaxation rates have been subtracted by the diamagnetic (1.0 mM HbO_2) contribution at any temperature.

CONCLUSIONS

The results reported in this paper definitely establish that the strong relaxation enhancement shown by the fluoride derivative of some hemoproteins is related to a water molecule hydrogen bonded to the heme iron coordinated fluoride ligand. The exchange lifetime of this second coordination sphere water molecule is short enough not to affect the R_{1p} values at any frequency for sperm whale Mb, horse Mb, and *C. caretta* Mb, whereas it increases to 2×10^{-6} in human Hb. In the latter case, the structure fluctuations of the globin folding may be partially hindered by the constraints occurring in the tetramer quaternary structure and may not allow the overall flexibility reported by the faster ligand exchange in Mb:fluoride adducts.

On the other hand, the fluoride ligand in *A. limacina* Mb is not involved in any interaction with water molecule(s) in the distal cavity (Conti et al., 1993), and the small enhancement of the solvent water proton relaxation rate is then associated only with an outer-sphere mechanism. As fluoride is replaced by formate anion, the stereochemical properties of the latter ligand do not allow any water molecule to closely approach the paramagnetic center (Leci et al., 1995) and then the observed relaxivity for all of the hemoproteins considered is quite similar and corresponds to the low values expected for systems where only the outer-sphere mechanism is operating.

A comparison of the binding modes of fluoride and formate to *C. caretta* Mb and sperm whale Mb, respectively, reveals that formate is actually replacing not just the fluoride anion but rather the F···H–OH moiety. In fact, whereas one oxygen atom of the formate ligand coordinated to the heme iron is hydrogen bonded to HisE7 NE2 (as fluoride ligand does), the second oxygen atom lies at the position occupied by the water oxygen (W195) in the fluoride derivatives. Interestingly, there is also a significant interaction between the W195 water molecule and the HisE7 residue that stabilizes the heme iron coordinated fluoride ion. Thus, we conclude that the presence of a histidyl residue in the E7 position plays a relevant role in bringing a water molecule close to the fluoride ion.

In *A. limacina* Mb, where HisE7 is replaced by Val, the binding of fluoride is still allowed, being the ligand stabilized by ArgE10; however, the latter residue is not as effective as HisE7 (given its location, size, and orientation) for the stabilization of a fluoride-bound water molecule. It follows that no water molecule is present in the second coordination sphere of the heme iron, and the observed relaxivity is similar to that observed for its ferric derivative (Giacometti et al., 1981) and for all of the formate adducts.

Authors thank Prof. M. Brunori and Prof. M. Paci for helpful discussions.

This work has been supported by grants from the Ministero dell'Università e della Ricerca Scientifica e Tecnologica of Italy, from the Centro Interuniversitario Studio Macromolecole Informazionali (University of Pavia, Italy), and from the Consiglio Nazionale delle Ricerche of Italy, Target Oriented Project "Biotecnologie e Biostrumentazione."

REFERENCES

Aime, S., P. Ascenzi, M. Fasano, and S. Paoletti. 1993. NMR relaxometric studies of water accessibility to haem cavity in horse heart and sperm whale myoglobin. *Magn. Res. Chem.* 31:S85–S89.

Aime, S., M. Fasano, S. Paoletti, A. Arnelli, and P. Ascenzi. 1995. NMR relaxometric investigation on human methemoglobin and fluoromethemoglobin. An improved quantitative in vitro assay of human methemoglobin. *Magn. Reson. Med.* 33:827–831.

Ansari, A., C. M. Jones, E. R. Henry, J. Hofrichter, and W. A. Eaton. 1994. Conformational relaxation and ligand binding in myoglobin. *Biochemistry.* 33:5128–5145.

Antonini, E., and M. Brunori. 1971. Hemoglobin and Myoglobin in Their Reactions with Ligands. Elsevier North-Holland Publishing Co., Amsterdam and London. 1–12, 40–54, 219–285.

Banci, L., I. Bertini, and C. Luchinat. 1991. Nuclear and Electron Relaxation. VCH, Weinheim.

Bashford, D., C. Clothia, and A. M. Lesk. 1987. Determinants of a protein fold: unique features of the globin amino acid sequences. *J. Mol. Biol.* 196:199–216.

Bertini, I., and C. Luchinat. 1986. NMR of Paramagnetic Molecules in Biological Systems. Benjamin/Cummings, Menlo Park.

Bolognesi, M., A. Coda, F. Frigerio, G. Gatti, P. Ascenzi, and M. Brunori. 1990. X-ray crystal structure of the fluoride derivative of *Aplysia limacina* ferric myoglobin at 2.0 Å resolution: stabilization of the fluoride ion by hydrogen bonding to Arg66 (E10). *J. Mol. Biol.* 213:621–625.

Brancaccio, A., F. Cutruzzolà, C. Travaglini Allocatelli, M. Brunori, S. J. Smerdon, A. J. Wilkinson, Y. Dou, D. Keenan, M. Ikeda-Saito, R. E. Brantley, Jr., and J. S. Olson. 1994. Structural factors governing azide and cyanide binding to mammalian metmyoglobins. *J. Biol. Chem.* 269:13843–13853.

Brünger, A. T. 1990. X-PLOR Manual: Version 2.1. Yale University, New Haven.

Brunori, M., M. Coletta, P. Ascenzi, and M. Bolognesi. 1989. Kinetic control of ligand binding processes in hemoproteins. *J. Mol. Liquids.* 42:175–193.

Conti, E., C. Moser, M. Rizzi, A. Mattevi, C. Lionetti, A. Coda, P. Ascenzi, M. Brunori, and M. Bolognesi. 1993. X-ray crystal structure of *Aplysia limacina* myoglobin in different liganded states. *J. Mol. Biol.* 233: 498–508.

Deatherage, J. F., R. S. Loe, and K. Moffat. 1976. Structure of fluoride methemoglobin. *J. Mol. Biol.* 104:723–728.

Fabry, M. E., and M. Eisenstadt. 1974. The mechanism of water proton nuclear magnetic resonance relaxation in the presence of mammalian and *Aplysia* metmyoglobin fluoride. *J. Biol. Chem.* 249:2915–2919.

Fann, Y., J. Ong, J. M. Nocek, and B. M. Hoffman. 1995. ^{19}F and $^{1,2}H$ ENDOR study of distal-pocket N(ε)-H···F hydrogen bonding in fluorometmyoglobin. *J. Am. Chem. Soc.* 117:6109–6116.

Fermi, G., and M. F. Perutz. 1977. Structure of human fluoromethaemoglobin with inositol hexaphosphate. *J. Mol. Biol.* 114:421–423.

Friebolin, H. 1993. Basic One- and Two-Dimensional NMR Spectroscopy. VCH, Weinheim.

Giacometti, G. M., P. Ascenzi, M. Brunori, G. Rigatti, G. Giacometti, and M. Bolognesi. 1981. Absence of water at the sixth co-ordination site in ferric *Aplysia* myoglobin. *J. Mol. Biol.* 151:315–319.

Gupta, R. K., and A. S. Mildvan. 1975. Nuclear relaxation studies on human methemoglobin. Observation of cooperativity and alkaline Bohr effect with inositol hexaphosphate. *J. Biol. Chem.* 250:246–253.

Hwang, L.-P., and J. H. Freed. 1975. Dynamic effects of pair correlation functions on spin relaxation by translational diffusion in liquids. *J. Chem. Phys.* 63:4017–4025.

Jones, T. A. 1978. A graphics model building and refinement system for macromolecules. *J. Appl. Crystallogr.* 11:268–272.

Koenig, S. H., and R. D. Brown, III. 1990. Field-cycling relaxometry of protein solutions and tissue: implications for MRI. *Prog. Nucl. Magn. Reson. Spectrosc.* 22:487–567.

Koenig, S. H., R. D. Brown, III, and T. R. Lindstrøm. 1981. Interactions of solvent with the heme region of methemoglobin and fluoromethemoglobin. *Biophys. J.* 34:397–408.

Leci, E., A. Brancaccio, F. Cutruzzolà, C. Travaglini Allocatelli, C. Tarricone, M. Bolognesi, A. Desideri, and P. Ascenzi. 1995. Formate binding to ferric wild-type and mutant myoglobins: thermodynamic and X-ray crystallographic study. *FEBS Lett.* 357:227–229.

Nardini, M., C. Tarricone, M. Rizzi, A. Desideri, A. Lania, G. De Sanctis, M. Coletta, R. Petruzzelli, P. Ascenzi, A. Coda, and M. Bolognesi. 1995. Reptile heme protein: X-ray crystallographic study of the aquo-met and cyano-met derivatives of the loggerhead sea turtle (*Caretta caretta*) myoglobin at 2.0 Å resolution. *J. Mol. Biol.* 247:459–465.

Noack, F. 1986. NMR field-cycling spectroscopy: principles and applications. *Prog. Nucl. Magn. Reson. Spectrosc.* 18:171–276.

Oakes, J. 1986. ^{1}H and ^{19}F nuclear magnetic resonance investigation of the active site of catalase. *J. Chem. Soc. (Faraday 1).* 82:2079–2087.

Perutz, M. F. 1979. Regulation of oxygen affinity of hemoglobin: influence of structure of the globin on the heme iron. *Annu. Rev. Biochem.* 48:327–386.

Perutz, M. F. 1989. Myoglobin and haemoglobin: role of distal residues in reactions with haem ligands. *Trends. Biochem. Sci.* 14:42–44.

Perutz, M. F. 1990. Mechanisms regulating the reactions of human hemoglobin with oxygen and carbon monoxide. *Annu. Rev. Physiol.* 52:1–25.

Smerdon, S. J., S. Krzywda, A. M. Brzozowski, G. J. Davies, A. J. Wilkinson, A. Brancaccio, F. Cutruzzolà, C. Travaglini Allocatelli, M. Brunori, T. Li, R. E. Brantley, Jr., T. E. Carver, R. F. Eich, E. Singleton, and J. S. Olson. 1995. Interactions among residues CD3, E7, E10 and E11 in myoglobins: attempts to simulate the ligand binding properties of *Aplysia limacina. Biochemistry.* 34:8715–8725.

Springer, B. A., S. G. Sligar, J. S. Olson, and G. N. Phillips, Jr. 1994. Mechanism of ligand recognition in myoglobin. *Chem. Rev.* 94: 699–714.

Takano, T. 1977. Structure of myoglobin refined at 2.0 Å resolution: crystallographic refinement of metmyoglobin from sperm whale. *J. Mol. Biol.* 110:537–568.

Vuk-Pavlovic, S., V. Bracika, B. Benko, and S. Maricic. 1977. A proton magnetic relaxation study of ferric myoglobin and haemoglobin in water/ethanediol solutions. *Biochim. Biophys. Acta.* 491:447–456.